2018 Annual American Control Conference (ACC)
June 27–29, 2018. Wisconsin Center, Milwaukee, USA

Modeling and Control of Web Lateral Dynamics in Roll-to-Roll Manufacturing: New Governing Equations and Control Strategies

Edison O. Cobos Torres and Prabhakar R. Pagilla*

Abstract— **In this paper we derive spatially dependent transfer functions for web lateral dynamics which provide web lateral position and slope at any location within the web span. This is a significant improvement over existing lateral transfer functions which provide the web lateral response only on the rollers. Our approach relies on taking the Laplace transform with respect to the temporal variable of both the web span lateral governing equation and the normal entry boundary conditions on the rollers, and solving the resulting equations. A general web span lateral transfer function, which is an explicit function of the spatial position along the span, is obtained. The new governing equations provide mechanisms to analyze web lateral behavior within spans, study propagation of lateral disturbances, and aid in the development of closed loop lateral control systems in emerging applications that require precise lateral positioning of the web. Both web lateral position and slope must be controlled to minimize propagation of lateral web oscillations into downstream spans. We illustrate the use of the new governing equations by providing numerical simulations for some representative disturbance and span scenarios.**

I. INTRODUCTION

In roll-to-roll (R2R) manufacturing, the focus of the work in modeling and control of webs (flexible materials) has been primarily in the longitudinal or transport direction. Web lateral dynamics and control (motion perpendicular to the transport direction and in the plane of the web) have not received as much attention. Increased use of R2R manufacturing in recent years (in flexible electronics and many conventional products) for processing a variety of web materials under different conditions has led to additional requirements of precisely controlling the lateral motion. For example, in R2R printing where patterns are sequentially printed on the web on multiple cylinders and registered, there have been stringent requirements on minimizing print registration in both longitudinal and lateral directions.

Studies on modeling the lateral behavior of moving webs date back to about 50 years. The first comprehensive work on the topic was reported by Shelton in [1], [2]. For the purpose of deriving the governing equations of the web lateral position on rollers, Shelton treated the moving web between two rollers as a tensioned Euler-Bernoulli beam. For most webs, the web mass is negligible, i.e., the force due to the acceleration of web mass is negligible when compared to web tension, and, thus, treating the problem as a continuous change of shape of a static beam. Four boundary conditions were considered (web lateral position and slope on each roller) to solve the differential equation describing the web lateral motion. A key observation/principle that was prevalent in the belt transport literature – a belt approaching a roller aligns itself normal to the axis of rotation of the roller – was used to setup two normal entry conditions for web lateral velocity and acceleration in terms of roller lateral velocity and acceleration, web slope at roller entry, and angle of the roller. Based on this approach, transfer functions were derived from the guide roller lateral position (input variable) to the web lateral position on the roller (controlled output variable) for various guide roller mechanisms. Subsequent work in modeling and control of web lateral dynamics based on this treatment was reported in [3]–[9]. A major drawback of the existing approach is the use of lateral transfer functions that provide web lateral position response only on the rollers.

The focus of this work is to remedy this problem. We derive a governing equation for web lateral motion and normal entry conditions by considering both bending and shear and clearly differentiating these effects. Our approach relies on taking the 1D Laplace transform of the span governing equation and the boundary conditions with respect to the temporal variable. The application of 1D Laplace transform for distributed parameter systems can be found in [10]. We consider the web lateral position and slope on the entry roller to the span as two boundary conditions and the two normal entry conditions (for lateral velocity and lateral acceleration) on the exit roller as the other two boundary conditions. The idea of incorporating the normal entry principles has been considered in [4] where these conditions are considered for a system modeled using a dynamic beam equation; a 2D Laplace transform (for both spatial and temporal variables) was applied to the governing equation; this provided a solution to the beam equation in the frequency domain. Due to the complexity of determining the inverse Laplace transform, the frequency domain solution was ignored and the spatial derivatives in the beam model were discretized using a finite difference method to obtain a set of ordinary differential equations for web lateral position response on the roller. Our approach allows us to solve the resulting equations, and obtain spatially dependent lateral transfer functions.

In web lateral control system, the measurement from a lateral position sensor that is located immediately downstream of the controlled guide roller is used as feedback for the controller. Although it has been recognized in the web handling community that the control of web slope is also critical to maintaining lateral position [3], [7], lack of

This work was supported the National Science Foundation under grant number 1635636.

*E. O. Cobos Torres and Prabhakar R. Pagilla are with the Department of Mechanical Engineering, Texas A&M University, College Station, TX 77843, U.S.A. Corresponding author email: ppagilla@tamu.edu.

governing equations that provide both web lateral position and slope along the span curtailed further work on this aspect. A guiding apparatus is presented in [7] where four displacement sensors were employed to solve four simultaneous equations to compute the coefficients of the lateral governing equations and calculate the web lateral position and slope. The approach presented in this paper allows us to obtain not only position but also slope at any location in the span; thus, eliminating the need for multiple sensors; one can also use the transfer function to control the web lateral position at any location along the span using a traditional, intermediate web guide. This is important for designing controllers for regulation of lateral position at any point in the span, and studying strategies that minimize propagation of lateral position and slope errors into downstream spans. Further, the derived functions can be applied to any guide configuration and specific transfer functions for those guiding situations can be determined.

The rest of the paper is organized as follows. In Section II, the governing equation for lateral behavior that includes shear and bending effects and normal entry conditions for the web are obtained. Then, using the governing equations a lateral transfer functions for various inputs that are functions of the transport direction spatial coordinate are derived. Control strategies and numerical simulations using this model are discussed in Section III. Concluding remarks are provided in Section IV.

II. MODELING

Figure 1 shows a web span with two adjacent rollers referred to as the entry and exit rollers. The web lateral positions are denoted by y_0 and y_L for the entry and exit rollers, respectively. The free span is the portion of the web between the rollers that is not in contact with them, and this length is denoted by L. The roller angle is denoted by θ, web speed transport by v, and the transport direction coordinate by x. In this section we develop spatially dependent transfer functions for web lateral position and slope by considering both bending and shear.

A. Governing Equation and Boundary Conditions

A section of the web considering both shear and bending is shown in 2, where T denotes web tension and θ_L is the angle.

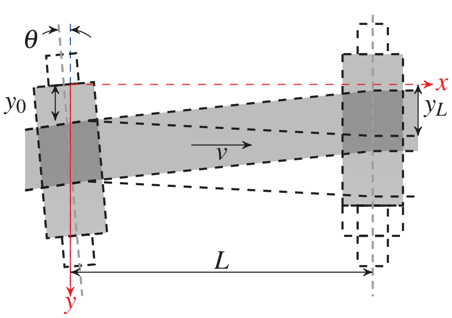

Fig. 1: Web span and notation

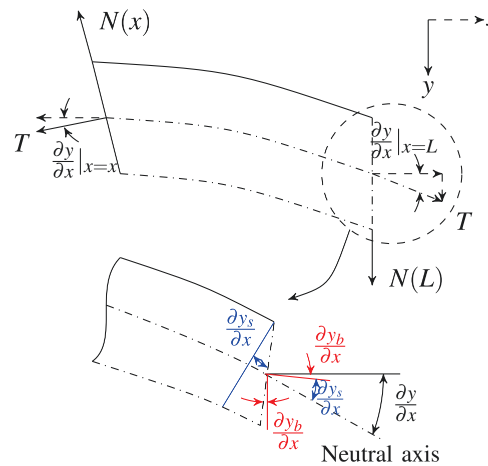

Fig. 2: Web section with bending and shear effects

The web slope due to the shear force $N(x)$ (considering the web span as a Timoshenko beam) can be expressed as

$$\frac{\partial y_s(x,t)}{\partial x} = \frac{nN(x)}{AG} \tag{1}$$

where n is a correction factor and equal to 1.2 for rectangular cross sectional area, A is the web cross sectional area, and G is the shear modulus. We will use subscripts b and s to refer to pure bending and pure shear, respectively, and no subscript to refer to the total deflection due to combined bending and shear. Considering the forces in Fig. 2, the shear force may also be expressed as

$$N(x) = T\left(\frac{\partial y(L,t)}{\partial x} - \frac{\partial y(x,t)}{\partial x}\right) + N(L). \tag{2}$$

Taking two consecutive derivatives with respect to x of Equations (1) and (2), and combining these two equations results in the following relationship:

$$\frac{\partial^3 y_s(x,t)}{\partial x^3} = -\frac{nT}{AG}\frac{\partial^3 y(x,t)}{\partial x^3}. \tag{3}$$

Further, from beam theory, the shear force is also given by

$$N(x) = -EI\frac{\partial^3 y_b(x,t)}{\partial x^3}. \tag{4}$$

Combining (3) and (4) and utilizing that the total web slope due to shear and bending is given by $\partial y/\partial x = \partial y_b/\partial x + \partial y_s/\partial x$, we can write

$$N(x) = -EI\left[1 + \frac{nT}{AG}\right]\frac{\partial^3 y(x,t)}{\partial x^3}. \tag{5}$$

Taking the partial derivative with respect to x and employing $\partial N(x)/\partial x = -T(\partial^2 y(x,t)/\partial x^2)$ (obtained from Equation (2)), one can establish the following governing equation for the web that includes both bending and shear:

$$\frac{\partial^4 y(x,t)}{\partial x^4} - K_e^2\frac{\partial^2 y(x,t)}{\partial x^2} = 0 \tag{6}$$

where $K_e^2 = (T/EI)/[1 + (nT/AG)]$. Notice that one can set $n = 0$ in (6) to obtain the pure bending case.

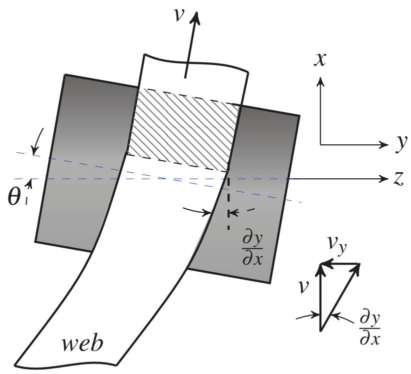

Fig. 3: Web behavior at roller entry

We require four boundary conditions to determine the solution for (6). They are deduced from the normal entry condition, i.e, the web immediately aligns perpendicular to the roller axis of rotation when it makes contact with the roller, which is illustrated in Fig. 3. Notice in this Figure that variable z represents the roller lateral displacement and it is used to differentiate it from the web lateral position. Two of the four boundary conditions are given at the entry roller ($x=0$) as,

$$y(0,t) = y_0(t); \quad \frac{\partial y(0,t)}{\partial x} = \theta_0(t). \tag{7}$$

The other two boundary conditions for the exit roller can be derived based on this normal entry condition, one based on lateral velocity and the other on lateral acceleration. We can obtain the following relationship between the web slope and roller lateral velocity (see Fig. 3), as the thrid boundary condition:

$$\frac{\partial y(L,t)}{\partial x} = \theta_L(t) + \frac{1}{v}\frac{\partial z_L(t)}{\partial t} - \frac{1}{v}\frac{\partial y(L,t)}{\partial t}. \tag{8}$$

To determine the fourth boundary condition, it is necessary to consider the following relationship for the rotational velocities [11]:

$$\frac{\partial \theta_L(t)}{\partial t} = \frac{\partial^2 y_b(L,t)}{\partial t \partial x} + v\frac{\partial^2 y_b(L,t)}{\partial x^2}. \tag{9}$$

Using $\partial y_b/\partial x = \partial y/\partial x - \partial y_s/\partial x$ in (9) and substituting the resulting equation in the time derivative of (8), we obtain the fourth condition boundary condition as

$$\frac{\partial^2 y(L,t)}{\partial x^2} = \frac{1}{v^2}\left(\frac{\partial^2 y(L,t)}{\partial t^2} - \frac{\partial^2 z_L(t)}{\partial t^2}\right) + \frac{1}{v}\left(\frac{\partial}{\partial t}\frac{\partial y_s(L,t)}{\partial x} + v\frac{\partial^2 y_s(L,t)}{\partial x^2}\right). \tag{10}$$

However, the above boundary condition for lateral acceleration is in terms of the shear angle. A relationship for shear angle ($\partial y_s/\partial x$) in terms of lateral displacement (y) would aid in determining the coefficients of the general solution of the governing equation. To find such a relationship, substitute the shear force expressed by (5) in (1) to obtain

$$\frac{\partial y_s(x,t)}{\partial x} = \frac{n}{AG}\left(-EI\frac{\partial^3 y(x,t)}{\partial x^3}\left[1+\frac{nT}{AG}\right]\right). \tag{11}$$

A Hamiltonian method is employed for finding such an expression in [9]. Now, using the definition of K_e^2 in (11) and substituting in (10), the fourth boundary condition for lateral acceleration at the exit roller can be written as

$$\frac{\partial^2 y(L,t)}{\partial x^2} = \frac{1}{v^2}\left(\frac{\partial^2 y(L,t)}{\partial t^2} - \frac{\partial^2 z_L(t)}{\partial t^2}\right) - \frac{nT}{vAGK_e^2}\left(\frac{\partial}{\partial t}\frac{\partial^3 y(L,t)}{\partial x^3} + v\frac{\partial^4 y(L,t)}{\partial x^4}\right). \tag{12}$$

Now, the governing equation and the boundary conditions are in terms of the total lateral displacement.

B. Lateral Transfer Functions

To solve the governing equation (6) with boundary conditions (7), (8), and (12), we apply the following 1D Laplace transform in the temporal variable:

$$\mathscr{L}\{f(x,t)\} = \hat{f}(x,s) = \int_0^\infty e^{-st} f(x,t)dt \tag{13}$$

to obtain,

$$\frac{\partial^4 \hat{y}(x,s)}{\partial x^4} - K_e^2\frac{\partial^2 \hat{y}(x,s)}{\partial x^2} = 0 \tag{14}$$

and

$$\begin{gathered}\hat{y}(0,s) = \hat{y}_0(s), \quad \frac{\partial \hat{y}(0,s)}{\partial x} = \hat{\theta}_0(s), \\ \frac{\partial \hat{y}(L,s)}{\partial x} = \hat{\theta}_L(s) + \frac{s}{v}\hat{z}_L(s) - \frac{s}{v}\hat{y}(L,s), \\ \frac{\partial^2 \hat{y}(L,s)}{\partial x^2} = \frac{s^2}{v^2}\left(\hat{y}(L,s) - \hat{z}(s)\right) - \frac{nTs}{vAGK_e^2}\left(\frac{\partial^3 \hat{y}(L,s)}{\partial x^3} - \frac{\partial^4 \hat{y}(L,s)}{\partial x^4}\right).\end{gathered} \tag{15}$$

The general solution for (14) is given by

$$\hat{y}(x,s) = C_{1e}(s)\sinh(K_e x) + C_{2e}(s)\cosh(K_e x) + C_{3e}(s)x + C_{4e}(s) \tag{16}$$

The coefficients $C_{ie}(s)$, $i=1,\ldots,4$, can be determined by using the boundary conditions given in (15). Once these coefficients are found, the solution (16) is given by

$$\hat{y}(x,s) = G_1(x,s)\hat{\theta}_0(s) + G_2(x,s)\hat{y}_0(s) + G_3(x,s)\hat{\theta}_L(s) + G_4(x,s)\hat{z}_L(s) \tag{17}$$

where

$$\begin{aligned} G_1(x,s) &= \frac{P_1(x,s)}{(\gamma s + (1+a)v)\left(s^2+bs+c\right)}\hat{\theta}_0(s), \\ G_2(x,s) &= \frac{P_2(x,s)}{\left(s^2+bs+c\right)}\hat{y}_0(s), \\ G_3(x,s) &= +\frac{P_3(x,s)}{(\gamma s + (1+a)v)\left(s^2+bs+c\right)}\hat{\theta}_L(s), \\ G_4(x,s) &= +\frac{P_4(x,s)}{(\gamma s + (1+a)v)\left(s^2+bs+c\right)}\hat{z}_L(s), \end{aligned} \tag{18}$$

$a = \frac{nT}{AG}$, $b = \frac{v((1+a)g_1(L)+\gamma)}{g_2(L)-g_3(L)}$, $c = \frac{v^2(1+a)}{g_2(L)-g_3(L)}$, $\gamma = \frac{a\sinh(K_eL)}{K_e(\cosh(K_eL)-1)}$,

$$g_1(x) = \frac{\sinh(K_eL)[\cosh(K_ex)-1] - \cosh(K_eL)[\sinh(K_ex)-K_ex]}{K_e[\cosh(K_eL)-1]},$$

$$g_2(x) = \frac{[\cosh(K_eL)-1][\cosh(K_ex)-1] - \sinh(K_eL)[\sinh(K_ex)-K_ex]}{K_e^2[\cosh(K_eL)-1]},$$

$$g_3(x) = a\frac{\sinh(K_eL)\left(\sinh(K_ex)-K_ex\right) - \cosh(K_eL)\left(\cosh(K_ex)-1\right)}{K_e^2\left(\cosh(KL)-1\right)},$$

$$P_1(x,s) = \frac{1}{(g_2(L)-g_3(L))}\Bigg[\Big(g_3(x)g_2(L)-g_2(x)g_3(L)+\gamma\Big(x\big(g_2(L)-g_3(L)\big)-L\big(g_2(x)-g_3(x)\big)\Big)\Big)s^3$$
$$+v\Big((1+a)\Big(\underbrace{(x-g_1(x))g_2(L)+(g_1(L)-L)g_2(x)}_{bending}+x(g_1(L)\gamma-g_3(L))-L(\gamma g_1(x)-g_3(x))\Big)+\gamma(x\gamma+g_3(x))\Big)s^2$$
$$+v^2(1+a)\Big(2x\gamma+g_3(x)-\gamma g_1(x)+(1+a)\underbrace{(xg_1(L)-Lg_1(x))}_{bending}\Big)s+(1+a)^2\underbrace{v^3(x-g_1(x))}_{bending}\Bigg] \quad (19)$$

$$P_2(x,s) = \frac{1}{(g_2(L)-g_3(L))}\Bigg[\Big(\underbrace{g_2(L)-g_2(x)}_{bending}-g_3(L)+g_3(x)\Big)s^2+v\Big(\gamma+(1+a)\underbrace{(g_1(L)-g_1(x))}_{bending}\Big)s+\underbrace{v^2}_{bending}(1+a)\Bigg] \quad (20)$$

$$P_3(x,s) = \frac{1}{(g_2(L)-g_3(L))}\Bigg[\Big(g_2(x)g_3(L)-g_3(x)g_2(L)\Big)s^3$$
$$+v\Big((1+a)\underbrace{(g_2(L)g_1(x)-g_1(L)g_2(x))}_{bending}-\gamma g_3(x)\Big)s^2+v^2(1+a)\Big(\gamma g_1(x)-g_3(x)\Big)s+(1+a)^2\underbrace{v^3g_1(x)}_{bending}\Bigg] \quad (21)$$

$$P_4(x,s) = \frac{1}{(g_2(L)-g_3(L))}\Big[\gamma(g_2(x)-g_3(x))s^3+v(1+a)(\underbrace{g_2(x)}_{bending}-g_3(x)+\gamma g_1(x))s^2+(1+a)^2\underbrace{v^2g_1(x)}_{bending}s\Big] \quad (22)$$

and $P_i(x,s)$, $i=1,\ldots,4$ are given in (19) through (22). To obtain the slope, moments or forces, it is necessary to take the first, second or third derivative with respect to x in (17), respectively. In the equations (19) to (22) for $P_i(x,s)$, the terms shown with under braces denote the contribution due to bending. Notice that if shear is not considered, then $\gamma=0$, $g_{3e}(x)=0$. Thus, Equation (17) is reduced to (23) [12]

$$\hat{y}(x,s) = \frac{P_4(x,s)}{s^2+v\frac{g_1(L)}{g_2(L)}s+\frac{v^2}{g_2(L)}}\hat{z}_L(s)+\frac{P_3(x,s)}{s^2+v\frac{g_1(L)}{g_2(L)}s+\frac{v^2}{g_2(L)}}\hat{\theta}_L(s)$$
$$+\frac{P_1(x,s)}{s^2+v\frac{g_1(L)}{g_2(L)}s+\frac{v^2}{g_2(L)}}\hat{\theta}_0(s)+\frac{P_2(x,s)}{s^2+v\frac{g_1(L)}{g_2(L)}s+\frac{v^2}{g_2(L)}}\hat{y}_0(s) \quad (23)$$

where

$$P_1(x,s) = \frac{1}{g_2(L)}\Big[((x-g_1(x))g_2(L)-(L-g_1(L))g_2(x))s^2 + v\big(xg_1(L)-Lg_1(x)\big)s+(x-g_1(x))v^2\Big]$$
$$P_2(x,s) = \frac{1}{g_2(L)}\Big[(g_2(L)-g_2(x))s^2+v(g_1(L)-g_1(x))s+v^2\Big]$$
$$P_3(x,s) = \frac{1}{g_2(L)}\Big[(g_1(x)g_2(L)-g_1(L)g_2(x))s^2+v^2g_1(x)\Big]$$
$$P_4(x,s) = \frac{1}{g_2(L)}\Big[g_2(x)s^2+vg_1(x)s\Big]$$

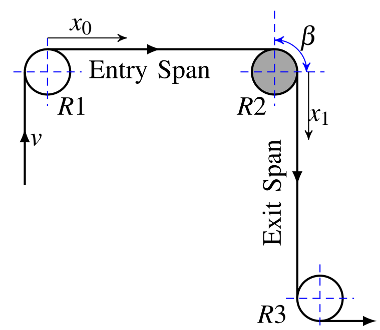

Fig. 4: Two span, three roller system

III. Control Strategies and Numerical Simulations

The benefits of our model in terms of control of web lateral position and slope via numerical simulations of a typical lateral guiding situation are discussed in this section. We will focus on control of both web lateral position and slope to reduce downstream propagation of lateral oscillations to spans. For this purpose, a commonly employed lateral guide called the Remotely Pivoted Guide (RPG) to control web lateral position is used. We consider a two-span, three-roller web setup shown in Fig. 4 where R2 is the guide roller (RPG) and R1 and R3 are pure idle rollers; we refer to the entry span as the 0-th span and the exit span as the 1-st span . The RPG roller R2 rotates around a pivot point in the entry span that is at a distance d_1 =0.7874 m from R2; since the RPG makes small roller angle changes for correcting the lateral position, the lateral displacement of the guide roller (R2) is related to the roller angle by, $z_L(t)=d_1\theta_L(t)$; see [5] for more details. Thus, the lateral response for any position in the entry span (L_0=1 m) is given by (17) with $z_L(t)=d_1\theta_L(t)$ and $\theta_L(t)$ as the control input. Similarly, one can also write down the lateral response in the exit span (L_1=1.16 m) using (17), with the respective values for that span.

Another key aspect is that when the exit span is not perpendicular to the entry span (wrap angle β not equal to 90°), then the exit span will see both bending and twist as a result of rotation of R2 in the plane of the entry span. If they are perpendicular, then only web twist is observed. The web slope at the beginning of the exit span is related to the roller angle by $\partial y(t)/\partial x\,|_{x_1=0}=\theta_L(t)\cos\beta$. Due to process conditions, it may not always be possible to maintain a wrap angle of 90° on R2. We consider the wrap angle on R2 to be 80° and employ Proportional and Integral (PI) controllers (industry practice) for all numerical simulations. A sinusoidal web lateral position disturbance of magnitude 2 mm on R1 is considered ($y_0 = 0.002\sin(3t)$) and control the lateral position in the exit span for the three cases given below. For each of the strategies, we are interested in observing oscillations in web lateral position and slope in the exit span. Numerical values of the web span and guide parameters used in the simulations are: reference tension T of 44.48 N, shear modulus G of $1.062 \times 10^9 Pa$, transport speed v=2.54 m/s, web thickness h of 0.127 mm, web width W of 137.16 mm, elastic modulus E=2.76×10^9 Pa [5].

Evolution of web lateral position and slope at 4 points along the entry and exit spans (see Fig. 4)

Entry Span | **Exit Span**, wrap angle of 80°

Case 1

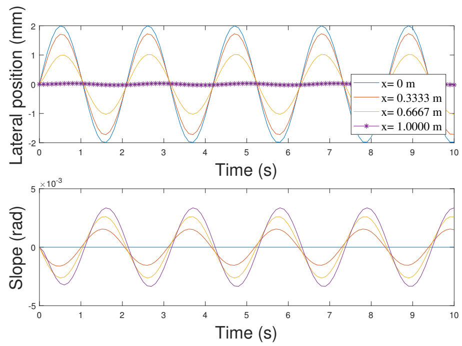

Fig. 5:

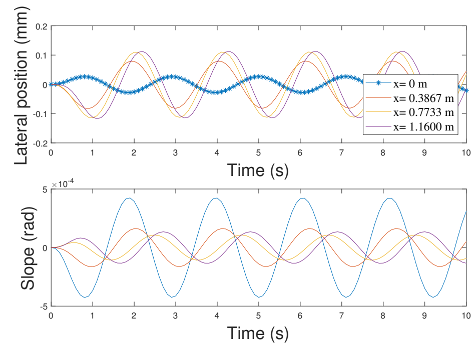

Fig.6:

Case 2

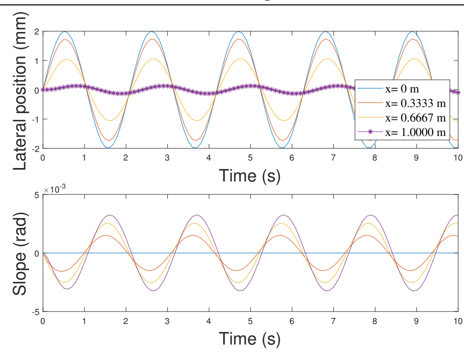

Fig. 7:

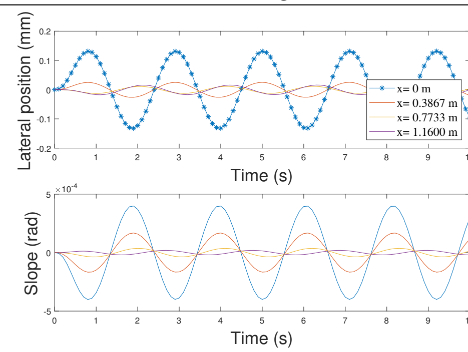

Fig. 8:

Case 3

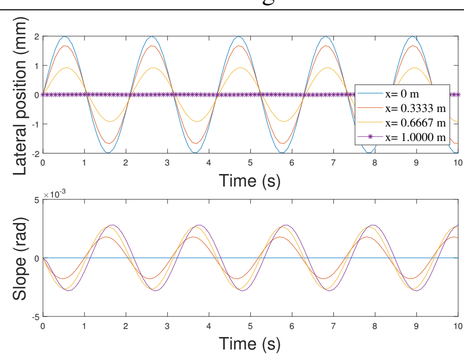

Fig. 9:

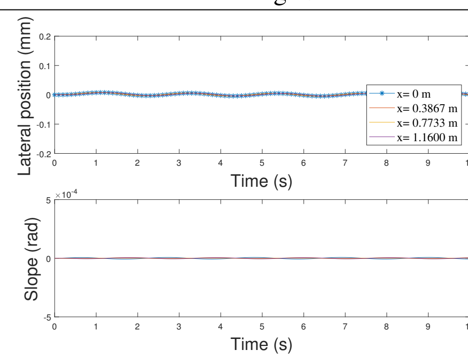

Fig. 10:

Case 1: In this case, we consider the existing industrial guide PI control strategy to control web lateral position on R2 with feedback from the sensor immediately downstream of R2, i.e., at $x_1 = 0$. Figure 5 provides the lateral position response for different locations in the entry span. It is clear that the web guide is able to regulate the web lateral position on roller R2, $y_L(t)$, to zero. This controller is typically considered as satisfactory in industrial practice as it provides very good lateral regulation on R2. Figure 6 provides the response of the lateral position and slope at different locations of the exit span to the disturbance. Although the lateral position at the guide roller has been regulated at zero, there is propagation of lateral oscillations into the downstream spans.

Case 2: In this case, we consider the control of web lateral position at a point $x_1 = L_1/3 = 0.3867$ m in the exit span length from R2 with lateral measurement at this point as feedback for the PI controller of the RPG. Figure 7 provides the position and slope for different points along the entry span for the controller downstream R2 with a wrap angle of 80°. The point of control is the second point in the exit span. The performance of this controller for the entry span differs from the previous controller as the web lateral position on the guide roller R2 is oscillatory. However, Fig. 8 shows that the controller is able to regulate the position at the prescribed point of interest. However, further oscillations are not eliminated.

Case 3: In this case, we consider control of web lateral position and slope independently by proposing a guide mechanism at roller R2 that enables such actions on the roller R2. It is assumed that both web lateral position and slope are measured at the point $x_1 = L_1/3 = 0.3867$ m and used as feedback for the respective PI controllers.Figures 9 and 10 show the response of the web lateral position and slope at four different points in the entry span and exit span, respectively, due to independent control of roller R2 angle and lateral position based on measurement of web lateral position and slope taken at the point x_1 in the exit span. It is clear from Fig. 10 that both the web lateral position and web slope are regulated at zero in the entire exit span, and further propagation of web lateral position or slope oscillations are not propagated downstream.

Note that control of lateral position and slope within in the spans (Cases 2 and 3) has been made possible due to the availability of the derived spatial dependent lateral transfer functions. The previous approach only provides the position on the rollers, which is represented in the simulations by the lines with the asterisk legend.

These numerical simulations on a typical web path in a R2R machine illustrate the benefit of the developed spatially dependent transfer functions for understanding lateral behavior in ideal as well as non-ideal situations.

IV. CONCLUSIONS

In this paper, we have derived new governing equations for web lateral behavior that are dependent on the spatial position along the span by considering both bending and shear. By employing normal entry conditions on the exit roller of the span as the boundary conditions, we incorporated the effect of web/roller contact into the solution of the governing equation. The obvious benefits are that one can obtain the evolution of lateral position response at any location in the span as well as all higher-order spatial partial derivatives, such as, slope, moment, shear force, etc., directly. In addition, R2R manufacturing of flexible and printed electronics requires positioning the web precisely in both lateral and longitudinal directions. Traditional printing systems have relied solely on longitudinal registration for printing presses with multiple print units. With the goal of achieving print registration accuracy to within a few microns in R2R printing of electronics, this work is expected to aid in a more precise analysis of lateral behavior and facilitate the design of model-based lateral control systems for achieving tight regulation of lateral print registration. Future work will consider design of model-based control algorithms for regulating both lateral position and slope as well as experimental validation. Experimental work on web lateral position and controllers based on previous models based on web lateral position on rollers has been widely reported. Our model reduced to the reported ones on the rollers, therefore those results apply to our case. However, information within the span has not been reported.

REFERENCES

[1] J. J. Shelton and K. N. Reid, "Lateral dynamics of a real moving web," *Transactions of the ASME, Journal of dynamics systems, measurements, and control*, vol. 93, no. 3, pp. 180–186, 1971.

[2] J. J. Shelton and K. N. Reid, "Lateral dynamics of an idealized moving web," *Transactions of the ASME, Journal of dynamics systems, measurements, and control*, vol. 93, no. 3, pp. 187–192, 1971.

[3] L. Sievers, *Modeling and Control of Lateral Web Dynamics*. Ph. D. Dissertation, Rensselaer Polytechnic Institute, Troy, NY., 1987.

[4] J. B. Yerashunas, J. A. D. Abreu-Garcia, and T. T. Hartley, "Control of lateral motion in moving webs," *IEEE Transactions on Control Systems Technology*, vol. 11, pp. 684–693, Sept 2003.

[5] A. Seshadri and P. R. Pagilla, "Optimal Web Guiding," *Transactions of the ASME, Journal of dynamic systems, measurement, and control*, vol. 132, no. 1, 2010.

[6] A. Seshadri and P. R. Pagilla, "Adaptive control of web guides," *Control Engineering Practice*, vol. 20, no. 12, pp. 1353 – 1365, 2012.

[7] R. Swanson, D. Carlson, J. Dobbs, and K. STENSVAD, "Apparatus for guiding a moving web," June 20 2013. WO Patent App. PCT/US2012/068,376.

[8] J. Brown, "A comparison of multispan lateral dynamic models," in *Proceedings of the Fourteen International Conference on Web Handling, Stillwater, OK, WHRC, Oklahoma State University*, Citeseer, 2015.

[9] J. Brown, "The effect of mass transfer on multi-span lateral dynamics of a uniform web," in *Proceedings of the Fourteenth International Conference on Web Handling, Stillwater, OK, WHRC, Oklahoma State University*, 2017.

[10] R. Curtain and K. Morris, "Transfer functions of distributed parameter systems: A tutorial," *Automatica*, vol. 45, no. 5, pp. 1101–1116, 2009.

[11] R. C. Benson, "Lateral dynamics of a moving web with geometrical imperfection," *Transactions of the ASME, Journal of dynamics systems, measurements, and control*, vol. 124, no. 1, pp. 25–34, 2002.

[12] E. O. Cobos Torres and P. R. Pagilla, "Spatially dependent transfer functions for web lateral dynamics," in *Proceedings of the Fourteenth International Conference on Web Handling, Stillwater, OK, WHRC, Oklahoma State University*, 2017.